

Research Article

In Silico Design of Novel Bioactive Molecules to Treat Breast Cancer with Uvaria Chamae Derivatives: A Computational Approach

Omobolaji Odunowo* 

College of Information, Information Science, University of North Texas, Denton, United States

Abstract

Breast cancer, which causes abnormal growth in breast tissue and can spread to other parts of the body, is difficult to treat due to the detrimental effects of traditional treatments such as radiation, chemotherapy, and surgery. Uvaria chamae a plant from the Annonaceae family, has antioxidant and antiproliferative characteristics, making it an alternative herbal treatment for cancer. The study aims to assess the bioactivity of Uvaria chamae leaf chemicals against the human placental aromatase in the breast cancer signaling pathway using a protein-ligand networking approach and molecular docking analysis. Bioactive Uvaria chamae compounds were downloaded from PubChem, examined for similarity using SWISS ADME, anticancer potential using PASSOnline, docked using PyRX, visualized with Biovia Discovery Studio, and tested for ADMET using pkCSM. Uvaria chamae leaves contain bioactive substances such as Apigenin, Diphenylcarbazide, Enamine, Naringin, Obovatin, Rutin trihydrate and Quercetin which have been shown to inhibit human placental aromatase proteins linked to breast cancer. Rutin trihydrate is a bioactive molecule that has a higher binding affinity than Exemestane which is used as reference drugs. The In silico analysis, drug likeness analysis, absorption, distribution, metabolism, excretion, and toxicity (ADMET) evaluation suggest that Rutin trihydrate, Quercetin and Apigenin derivatives from Uvaria chamae is a promising human placental aromatase inhibitor for breast cancer, with a binding affinity of -9.2, -8.0, and -8.0 kcal/mol compared to Exemestane (-7.5 kcal/mol). Considering the results of molecular docking, drug likeness analysis, absorption, distribution, metabolism, excretion, and toxicity (ADMET) evaluation, it can be concluded that Rutin trihydrate Quercetin and Apigenin derivatives hold promise as potent inhibitors for the treatment of breast cancer.

Keywords

Molecular Docking, Uvaria Chamae, Breast Cancer, Drug Development, Pharmacokinetic, *In silico* Design, ADMET, Human Placental Aromatase

1. Introduction

Cancer is a massive collection of disorders that can begin anywhere in the body and spread to other places when aberrant cells multiply and expand uncontrollably [1]. It is one of

the leading causes of death worldwide, and the incidence rate is increasing daily. It is one of the leading causes of death worldwide, and its incidence is rapidly increasing. According

*Corresponding author: omobolajiodunowo@gmail.com (Omobolaji Odunowo)

Received: 13 March 2025; **Accepted:** 25 March 2025; **Published:** 17 April 2025



Copyright: © The Author(s), 2025. Published by Science Publishing Group. This is an **Open Access** article, distributed under the terms of the Creative Commons Attribution 4.0 License (<http://creativecommons.org/licenses/by/4.0/>), which permits unrestricted use, distribution and reproduction in any medium, provided the original work is properly cited.

to a World Health Organization research, cancer is the top cause of mortality, accounting for almost 10 million fatalities in 2020, or one out of every six deaths [2]. The most prevalent cancer types include breast, lung, brain, colon, blood, prostate, stomach, and liver cancer. However, it is worth noting that breast, lung, and thyroid cancers are more common in women [3, 4]. In 2020, the most prevalent cancer diagnoses were breast cancer (2.26 million), lung cancer (2.21 million), colon and rectal cancer (1.93 million), prostate cancer (1.41 million), non-melanoma skin cancer (1.20 million), and stomach cancer (1.09 million). Among these, breast cancer was more closely associated with the female gender, accounting for 685,000 fatalities worldwide in 2020. Women aged 40 to 60 were more sensitive to breast cancer, accounting for roughly 75% of cases. Females under the age of 30 had only a 5% probability of developing breast cancer, while those over the age of 60 accounted for 20% of instances. According to these findings, the 40-60 age group has the highest incidence of breast cancer [5, 6].

Breast cancer can develop in any of the three main components of the breast: connective tissue, ducts, and lobules. In most cases, it starts in the epithelial cells of the ducts (85%) or lobules (15%) in the glandular tissue of the breast, where there are no symptoms (no metastases). It eventually spreads to nearby lymph nodes (regional metastasis) or other body parts (distant metastases). Breast cancer is divided into various types based on the affected cells [7-11]. The most used cancer treatments are chemotherapy, surgery, and radiotherapy, but they have substantial side effects on host cells, spurring the search for innovative alternatives [12]. To overcome the limitations of current chemotherapeutics, researchers concentrated on developing natural compounds as chemotherapeutic agents [13-15].

While many anticancer medications have come from natural sources, it is crucial to note that many plant molecules with anticancer properties are still relatively unexplored in drug discovery. Despite the accomplishments of natural anticancer agents, many plant elements have yet to be thoroughly studied for their medicinal potential. Phytochemicals may be employed as alternatives to synthetic chemotherapeutic treatments since they have anticancer properties and can preserve important cellular components such as DNA, proteins, and lipids from oxidation [16-18]. *Acanthus montanus* is a substantial family of flowering plants, encompassing more than 4,300 species and 346 genera worldwide [19]. The majority are tropical shrubs, herbs, and twining vines, while some are epiphytes, making it one of the world's top 12 most diversified flowering plant families. Various research has confirmed that the bioactive constituents of *Acanthus montanus*, has been use in the treatment of wounds, furuncles, gonorrhea, syphilis, cardiac dysfunction, diabetes with little work done on its effects in treatment of Cancer. Research has been conducted to determine the chemical composition of *Uvaria chamae*.

Gas chromatography-mass spectrometry (GC-MS) and

High performance liquid chromatography (HPLC) is widely used in metabolomics research to ensure the integrity of natural products and assess plant tolerance to abiotic stress. [20] found that GC-MS and HPLC analysis provides useful insights on plant pharmacology.

In silico molecular docking, a computational method used in drug discovery and design, is a useful tool for analyzing chemical compounds' binding affinities and spatial arrangement with protein targets [21]. This study aimed to evaluate the anti-cancer properties of ethanolic root extract of *Acanthus montanus* and its potential utility in breast cancer therapy.

2. Materials and Methods

2.1. Collection of Plant Materials

Uvaria chamae was collected from Oyo town, Oyo South Local Government Area, Oyo State, situated in the south-western region of Nigeria, characterised by a tropical savanna climate favourable for the growth of *Uvaria chamae*, the plant was harvested during its flowering season to ensure maximum phytochemical content. Details of the collection site, including geographical coordinates (latitude and longitude), were documented to allow reproducibility and traceability. The collected plant samples were examined for their distinguishing morphological features, such as leaves, fruits, and flowers, to ensure accurate species identification.

The initial identification was carried out by local experts familiar with the region's flora and was confirmed by a taxonomist at the Department of Plant Biology and Biotechnology, University of Benin, Nigeria. A representative specimen of *U. chamae* was prepared and preserved following standard herbarium protocols. This involves: Pressing and drying the plant material between blotting or newspaper sheets and mounting it on herbarium sheets with detailed labels, including the plant's local name, collection site, date, and collector's information. The voucher specimen will be deposited at the Herbarium unit of the department for future reference under an assigned accession number.

2.2. Preparation of the Extract

Fresh leaves of *Uvaria chamae* were collected, rinsed with distilled water to remove dirt and debris, and air-dried in a well-ventilated, shaded area to preserve bioactive compounds. The dried plant material was ground into a fine powder using a mechanical grinder to increase the surface area for extraction. A pre-determined quantity of the powdered plant material (e.g., 500 g) was weighed using an analytical balance and an aqueous solvent was used for the extraction. The powdered material was soaked in distilled water at a ratio of 1:10 (w/v; 500 g in 5 L of distilled water) in an airtight container to prevent evaporation and the mixture was intermittently stirred to enhance the dissolution of phytochemicals in water. This soaking process was carried out for 48–72 hours at room

temperature [22].

After the extraction period, the mixture was filtered using a muslin cloth or Whatman No. 1 filter paper to separate the aqueous extract from plant debris. The process was repeated for better yield by re-soaking the residue for another 24 hours. The filtered aqueous extract was concentrated under reduced pressure using a rotary evaporator at 40–50 °C to remove the solvent, leaving behind a semi-solid or dry crude extract. The crude extract was further dried in a vacuum oven or desiccator to eliminate residual solvent. The dried aqueous extract was then weighed, stored in an airtight container, and kept at 4 °C in a refrigerator until further analysis and a small portion of the extract was analyzed for preliminary phytochemical screening to confirm the presence of target bioactive compounds [22].

2.3. Gas Chromatography-mass Spectrometry (GC-MS) Analysis

The leaves of *Uvaria chamae* were analyzed using Gas

Chromatography-Mass Spectrometry. A GC-MS (Model; Agilent technologies 7890A) equipped with a VF - 5 ms fused silica capillary column of 30 m length, 0.25 mm diameter, and 0.25 mm film thickness was used. An electron ionization system with an ionization energy of 70eV was used for GC-MS detection. At a constant flow rate of 1 ml/min, helium gas (99.99%) was used as a carrier gas. The injection and mass transfer lines were set to 200 and 240 °C, respectively. The oven's temperature range was set to hold between 80 °C for 2 min at 10 °C/min and 240 °C for 6 min. Manually inserting 2 ml of water solution from the samples in split-less mode with a split ratio of 1:40 and a mass scan of 50–600 amu. The GC-MS ran for 35 min in total. Peak area normalization was used to express each extract constituent's relative percentage as a percentage. The National Institute of Standard and Technology (NIST) library's database, which contains more than 62,000 spectral patterns, was used to interpret the mass spectra of the plant extracts. The compounds' spectra and those of the National Institute of Standards and Technology were compared (Figure 1).

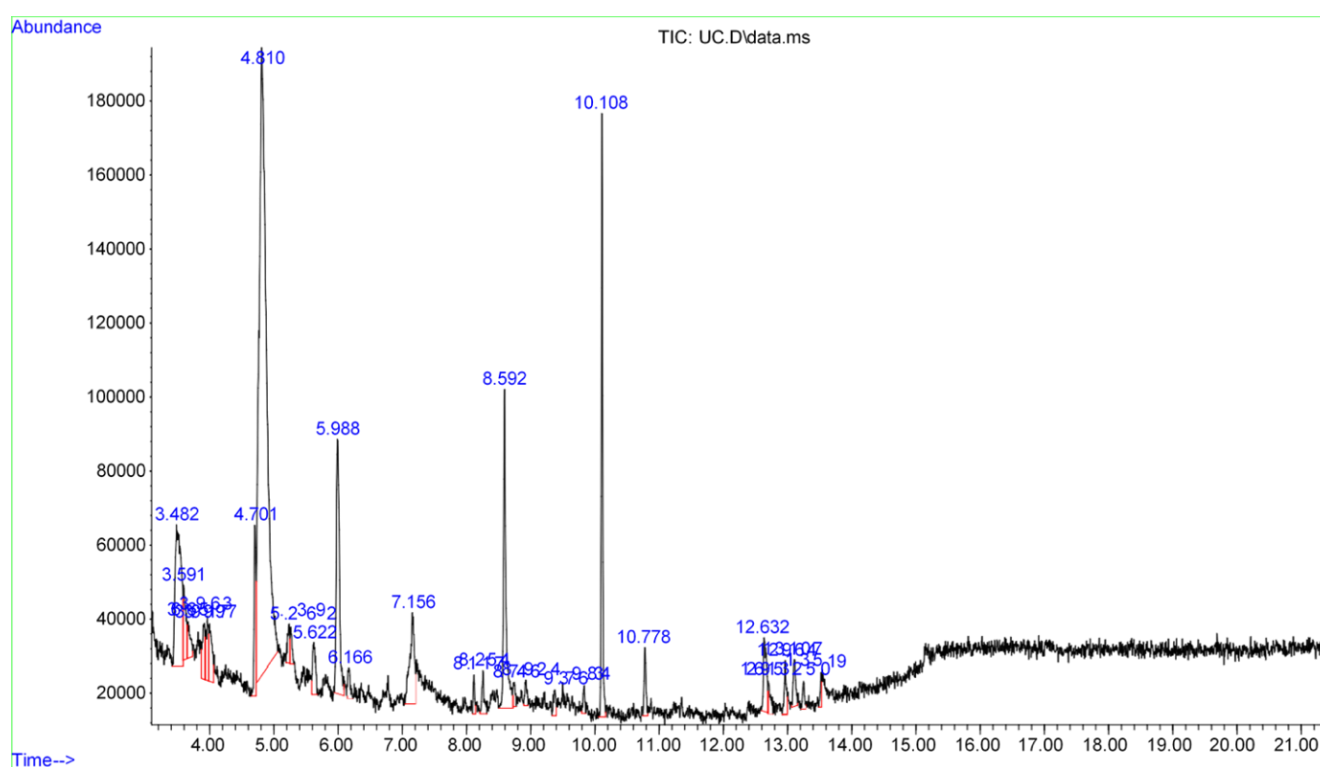


Figure 1. Graph showing the various peaks from the GC-MS analysis of *Uvaria chamae* leave.

2.4. High-performance Liquid Chromatography (HPLC) Analysis

The phytochemical analysis of *Uvaria chamae* extract was carried out using a High-performance liquid chromatography (HPLC). HPLC analysis of the extract was performed using

an Agilent 1260 Infinity II series equipped with DAD WR G71115A (DEAC606992), Column Oven of G7130 (DE-AEQ22974), Quat Pump VL G711A (DEAEY01907). Auto Sampler G7129A (DEAEQ22974) produced in the USA; and with a poroshell column 120 EC-C 18 4 µm (250 mm x 4.0 mm), PN 693970-902 (T), SN USHKB12136, LN B18447. During the HPLC experiment, a high-pressure pump takes the mobile phase from a reservoir through an injector. It then

travels through a reverse-phase C18-packed column for component separation. Finally, the mobile phase moves into a detector cell, where the absorbance is measured at 250 nm, and ends in a waste bottle. The amount of time it takes for a component to travel from the injector port to the detector is called the retention time. In this analysis, samples were injected into the HPLC system and eluted isocratically at a flow rate was 2 ml/min. The column dimensions are 250 mm x 4.0 mm. Detection is by absorption spectroscopy at a wavelength of 280 nm. The resulting chromatogram has a peak for every component in the sample. For this experiment, the mobile phase is primarily 20% acetonitrile and 80% purified deionized (DI) water. A small amount of acetic acid is added to lower the pH of the mobile phase, which keeps the silanol in the stationary packing phase in an undissociated state. This reduces the adsorption peak from tailing, giving narrower peaks. Then, the pH is adjusted with 40% sodium hydroxide to raise the pH and help decrease the retention times of the components.

2.5. Protein Optimization

The crystal structure of human placental aromatase complexed with the breast cancer drug exemestane domain [23] (PDB ID: 3S7S) was obtained from the protein data bank (<http://www.rcsb.org>). Human aromatase (Accession: NP_1125031_X GI: 281307079) "Fasta" file was retrieved from www.ncbi.nlm.nih.gov/pubmed and utilized to model the beginning structure of aromatase employed in the current investigation. The homology modeling was done using the Swiss Model Server (<http://swissmodel.expasy.org>). The 3D structure of aromatase was modeled using the coordinate file of a template from the protein data bank (PDB ID: 3S7S). Water and ligand coordinates were removed prior to molecular docking. In this experiment, Discovery Studio 2024 was used to remove the native ligand so the tested compounds could access the target protein's active sites later in the docking procedure. Subsequently, we determined the coordinates ($X = -10.729204$, $Y = 12.417653$, and $Z = 68.816122$) of the active site, and ultimately, we integrated the polar hydrogen into this structure.

2.6. Starting Coordinates: Uvaria Chamae Leaves Secondary Metabolites

Thirty-five phytochemicals from *Uvaria chamae* leaves were retrieved from the GC-MS and HPLC analysis. Exemestane, an FDA-sanctioned therapeutic agent, acting as the control. The three-dimensional (3D) structures of these ligands were acquired in simple data format (SDF) from the PubChem server through Open Babel in PyRx (version 0.8). This procedure energetically optimized the ligands into their most stable conformations using the Merck Molecular Force Field 94 (MMFF94).

2.7. Molecular Docking

A flexible docking approach, as outlined by Trott and Olson [24], was utilized to perform the molecular docking with minor modifications. The molecular docking analysis of the chosen ligands with the target protein was performed with PyRx (version 0.8), which integrates Auto Dock Vina. The PDBQT files for the proteins were generated utilizing their previously established PDB files as inputs. The receptor was made stiff by allowing all the ligand's linkages to rotate freely and adjusting the grid box to align with the protein molecule's active sites. Text files with score results were prepared to enable manual comparative analysis following completion of the molecular docking investigations, with ten configurations established for each protein-ligand interaction across all phytocompounds. Minimum binding energy (BE, kcal/mol).

2.8. Pharmacokinetic Screening

The highest-scoring compounds underwent structure-based pharmacokinetic screening to forecast their absorption, distribution, metabolism, excretion, and toxicity (ADMET) characteristics and drug likeness. Online servers ADMETlab 2.0 [25] was utilized to predict the key physicochemical properties that influence drug-likeness. The predicted properties include lipophilicity, water solubility, blood-brain barrier permeation, gastrointestinal absorption, and cytochrome P450 inhibition, among others.

3. Result

3.1. Molecular Docking and Binding Energy Analysis

From a total of Thirty-five natural compounds (Table 1), seven compounds were selected based on their superior binding affinity to the receptor: Apigenin (ID: 5280443), Diphenylcarbazide (ID: 8789), Enamine (ID: 555174), Naringin (ID: 442428), Obovatins (ID: 13940733), Rutin trihydrate (ID: 5280805) and Quercetin (ID: 5280343). The ligand docking scores for the receptor (PDB ID: 3S7S), the top seven lead compounds, and the corresponding standard drugs as approved by the Food and Drug Administration (FDA), are also presented in Table 1. Rutin trihydrate exhibited the highest docking score (-9.2). The subsequent six compounds were Apigenin, Enamine, Naringin, Diphenyl carbazide, Quercetin and Obovatins, with docking scores of -8.0, -7.2, -8.7, -7.2, -8.0 and -8.0, respectively. The standard drugs had a docking score of -7.5, markedly inferior to the lead compounds.

Table 1. Summary of molecular docking result.

No.	Compound name	Molecular formulae	Molecular Weight	Binding score (Kcal/mol)
1.	Phenol	C ₆ H ₆ O	94.11 g/mol	-5.5
2.	3-Methylpyridazine	C ₅ H ₆ N ₂	94.11 g/mol	-4.8
3.	Imidazo[1,5-a]pyrimidine	C ₆ H ₅ N ₃	119.12 g/mol	-5.1
4.	1-Phenylaziridine	C ₈ H ₉ N	119.16 g/mol	-5.5
5.	Methyl benzoate	C ₈ H ₈ O ₂	136.15 g/mol	-6.0
6.	Tricyclo(3.2.1.01,5)octane	C ₈ H ₁₂	108.18 g/mol	-4.7
7.	2-Methyl-1-hepten-3-yne	C ₈ H ₁₂	108.18 g/mol	-4.7
8.	6-Amino-6-methylfulvene	C ₇ H ₉ N	107.15 g/mol	-5.2
9.	3-Methylenecycloheptene	C ₈ H ₁₂	108.18 g/mol	-5.8
10.	2-Bromo-4,6-Difluoroaniline	C ₆ H ₄ BrF ₂ N	208.00 g/mol	-4.7
11.	2-Methylbenzyl alcohol	C ₈ H ₁₀ O	122.16 g/mol	-6.0
12.	4-Phenyloxazolidin-2-one	C ₉ H ₉ NO ₂	163.17 g/mol	-6.0
13.	Tetrazolo[1,5-a]pyridine-5-carboxylic acid	C ₆ H ₄ N ₄ O ₂	164.12 g/mol	-5.8
14.	Silane, trimethyl(3,5-xylyloxy)-	C ₁₁ H ₁₈ OSi	194.34 g/mol	-4.6
15.	Pent-2-ynal, 4,4-dimethyl-	C ₇ H ₁₀ O	110.15 g/mol	-4.3
16.	2,4-Dichloro-2',5'-dimethylbiphenyl	C ₁₄ H ₁₂ Cl ₂	251.1 g/mol	-6.8
17.	Isolongifolan-8-ol	C ₁₅ H ₂₆ O	222.37 g/mol	
18.	3-Nitrostyrene	C ₈ H ₇ NO ₂	149.15 g/mol	-5.7
19.	Aromadendrene, dehydro-	C ₁₅ H ₂₂	202.33 g/mol	-6.9
20.	Enamine_005840	C ₁₄ H ₁₄ O ₃	230.26 g/mol	-7.2
21.	Diphenylcarbazide	C ₁₃ H ₁₄ N ₄ O	242.28 g/mol	-7.2
22.	2-(Imidazo[1,2-a]pyridin-2-yl)acetonitrile	C ₉ H ₇ N ₃	157.17 g/mol	-5.6
23.	3-Octen-5-yne, (Z)-	C ₈ H ₁₂	108.18 g/mol	-4.6
24.	3-Methoxy-1,3,4-hexatriene	C ₇ H ₁₀ O	110.15 g/mol	-4.5
25.	Methyl nonanoate	C ₁₀ H ₂₀ O ₂	172.26 g/mol	-4.8
26.	Apigenin	C ₁₅ H ₁₀ O ₅	270.24 g/mol	-8.0
27.	Caffeic Acid	C ₉ H ₈ O ₄	180.16 g/mol	-6.2
28.	Ferulic Acid	C ₁₀ H ₁₀ O ₄	194.18 g/mol	-6.8
29.	Gallic Acid	C ₇ H ₆ O ₅	170.12 g/mol	-6.0
30.	Maleic acid	C ₄ H ₄ O ₄	116.07 g/mol	-5.3
35.	Naringin	C ₂₇ H ₃₂ O ₁₄	580.5 g/mol	-8.7
36.	Obovatin	C ₂₀ H ₁₈ O ₄	322.4 g/mol	-7.9
37.	p-Coumaric acid	C ₉ H ₈ O ₃	164.16 g/mol	-4.3
38.	Quercetin	C ₁₅ H ₁₀ O ₇	302.23 g/mol	-8.0
39.	Rutin trihydrate	C ₂₇ H ₃₆ O ₁₉	664.6 g/mol	-9.2
40.	Salicylic Acid	C ₇ H ₆ O ₃	138.12 g/mol	-6.1
	STANDARD/CONTROL			

No.	Compound name	Molecular formulae	Molecular Weight	Binding score (Kcal/mol)
1.	Exemestane	C ₂₀ H ₂₄ O ₂	296.4 g/mol	-7.5

The lead compounds exhibited robust interactions with the target compared to the standard drug. Figure 2 illustrates the 2D interaction profile of the receptor with the lead compounds. In the interaction with the amino acid residues in the ligand-binding domain of the receptor, Rutin trihydrate demonstrated a docking score of -9.2 kcal/mol and established hydrogen bond interactions with PRO 429, VAL 422, ASN 421, LYS 354, MET 444, TYR 441, ASN 358 and LYS 440. Quercetin established hydrogen bond interactions with ARG 403, LEU 479, PRO 368, GLN 367 and LYS 473. Furthermore, Enamine formed connections via hydrogen bonds with VAL 422 and PRO 429. Apigenin interacted with adjacent amino acids by hydrogen bonds with LYS 473, ASN 75, LEU479, GLN 367, and PRO 368. Obovatin formed connections via hydrogen bonds with ASN 421, VAL

422, TYR 361, GLU 357 and PRO 429. Naringin formed connections via hydrogen bonds with VAL 370, VAL 369, MET 364, PHE 430, MET 311, ALA 307, ALA 306, CYS 437 and ARE 115 as shown in Figure 3.

Rutin trihydrate demonstrated the highest binding energy to the receptor, with a ΔG value of -9.2 kcal/mol. Additionally, the Obovatin demonstrated binding energy of -7.9 kcal/mol. Apigenin and Quercetin demonstrated impressive free energy values of -8.0 kcal/mol. Additionally, Enamine demonstrated significant binding energy -7.2 kcal/mol, Diphenyl carbazide demonstrated a binding energy of -7.2 kcal/mol, all compared to the standard or control ligand Exemestane with a binding energy of -7.5 kcal/mol. The binding poses of the selected compound are shown in Figure 4.

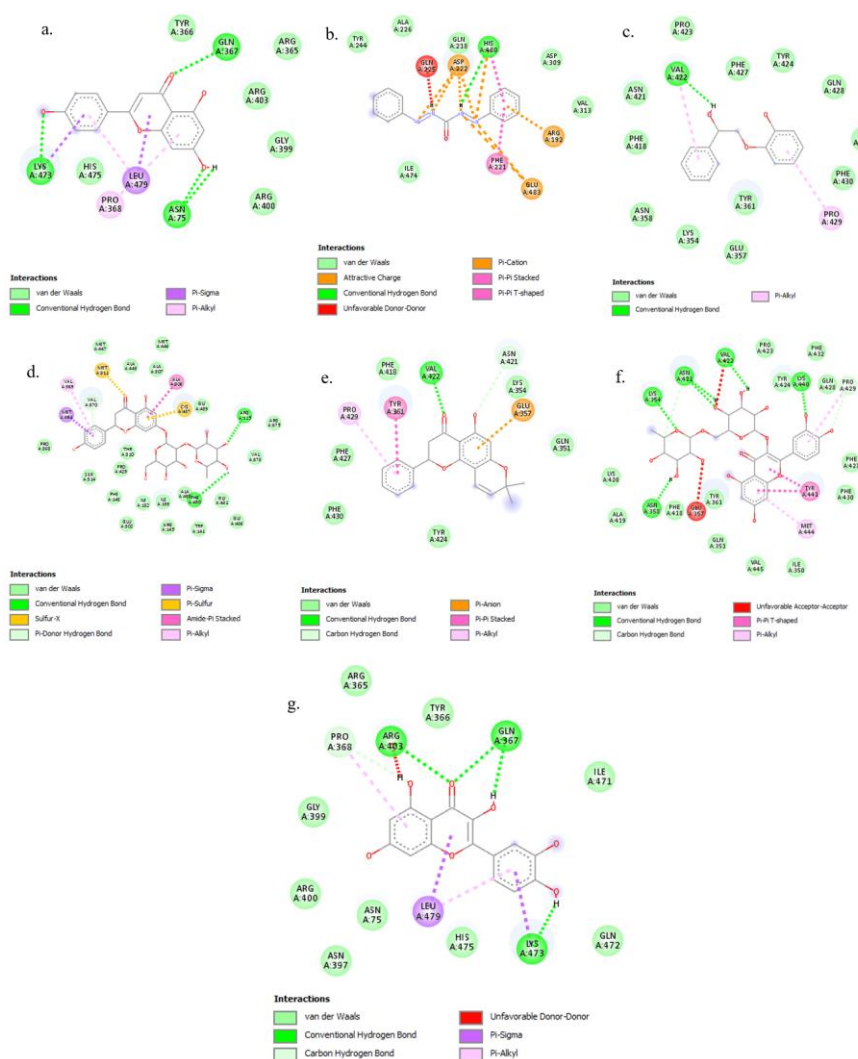


Figure 2. 2D view of the molecular interaction of the top seven compounds: (a.) Apigenin, (b.) Diphenyl carbazide, (c.) Enamine, (d.) Naringin, (e.) Obovatin, (f.) Rutin hydrate, (g.) Quercetin.

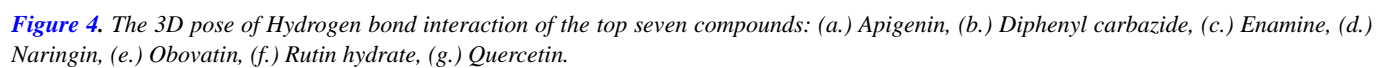
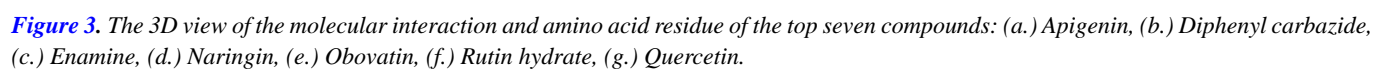


Table 2. Lipinski's rule of Six for the phytoconstituents in *Uvaria chamae*.

No.	Compound	MW ≤500 Dalton	nHA ≤10	nHD ≤5	logP ≤5	No. of rule violations ≤ 2 violations	Drug-Likeness
1.	Apigenin	270.05	5.0	3.0	2.981	0	Yes
2.	Diphenylcarbazine	242.12	5.0	4.0	1.353	0	Yes
3.	Enamine	242.05	2.0	5.0	1.345	0	Yes
4.	Naringin	580.18	14.0	8.0	0.475	3	No
5.	Obovatn	322.12	4.0	1.0	4.475	0	Yes
6.	Rutin trihydrate	610.15	16.0	10.0	0.986	3	No
7.	Quercetin	302.04	7.0	5.0	2.155	0	Yes

3.2. ADME-T Results

The outcomes of the in silico ADME-T analysis of phytoconstituents in *Uvaria chamae* are presented in Tables 2-6. The findings from the human intestinal absorption (HIA) test demonstrated that only Apigenin, Obovatn, Quercetin and Rutin trihydrate out of the seven selected compound exhibited high permeation across the membrane. (Table 3). In the in vitro Caco-2 cell permeability test, Enamine, Diphenylcarbazine, Apigenin and Obovatn demonstrated good permeation, except for Rutin trihydrate, Quercetin and Naringin. All compounds are anticipated to be soluble in water. All compounds exhibit distinct subcellular localization. All compounds demonstrated no inhibition of P-glycoprotein (P-gp) except Obovatn, and All

compounds were identified as P-gp substrates except Naringin. All compounds demonstrated a positive permeable to the blood-brain barrier (BBB). Enamine, Naringin and Rutin trihydrate are found to be non-inhibitors for CYP450 1A2, CYP450 2C9, CYP450 2D6, CYP450 2C19 and CYP450 3A4 (Table 5). Diphenylcarbazine and Apigenin acted as inhibitors for CYP1A2 and, CYP450 2D6. Obovatn acted as inhibitors for CYP450 2C9 and CYP450 2C19. All compounds demonstrated a lack of hepatotoxicity except Obovatn, and Naringin (Table 6). Diphenylcarbazine, Obovatn, Rutin trihydrate and Naringin exhibit mutagenic properties, as indicated by the AMES toxicity test. Several compounds were found to be non-carcinogenic. This analysis demonstrates that Quercetin, Apigenin and Enamine exhibit superior pharmacokinetic and toxicity profiles compared to other compounds.

Table 3. Absorption prediction output.

No.	Compound	Caco-2 Permeability	HIA	logS	Pgp-inhibitor	Pgp-substrate	Conclusion
1.	Apigenin	-5.129	0.002	-4.216	0.004	0.312	Yes
2.	Diphenylcarbazine	-4.788	0.736	-2.387	0.676	0.0	No
3.	Enamine	-4.785	0.913	-2.64	0.001	0.557	Yes
4.	Naringin	-6.764	0.751	-2.353	0.0	0.74	No
5.	Obovatn	-4.849	0.0	-5.043	0.993	0.006	Yes
6.	Rutin trihydrate	-6.547	0.64	-2.397	0.0	0.699	No
7.	Quercetin	-5.204	0.014	-3.671	0.004	0.005	Yes

Table 4. Distribution prediction output.

No.	Compound	BBB	BCRP inhibitor	MRP1 inhibitor
1.	Apigenin	0.013	0.892	0.657

No.	Compound	BBB	BCRP inhibitor	MRP1 inhibitor
2.	Diphenylcarbazine	0.0	0.0	0.011
3.	Enamine	0.018	0.006	0.923
4.	Naringin	0.0	0.843	0.07
5.	Obovat	0.357	0.924	0.937
6.	Rutin trihydrate	0.0	0.834	0.008
7.	Quercetin	0.008	0.099	0.008

Table 5. Metabolism prediction output.

No.	Compound	CYP450 1A2 inhibitor	CYP450 2C9 inhibitor	CYP450 2D6 inhibitor	CYP450 2C19 inhibitor	CYP450 3A4 inhibitor	Conclusion
1.	Apigenin	1.0	0.002	0.957	0.112	1.0	No
2.	Diphenylcarbazine	0.996	0.229	0.773	1.0	0.968	No
3.	Enamine	0.0	0.0	0.0	0.0	0.0	Yes
4.	Naringin	0.0	0.087	0.0	0.0	0.0	Yes
5.	Obovat	0.0	0.999	0.003	0.999	0.239	No
6.	Rutin trihydrate	0.0	0.0	0.0	0.0	0.0	Yes
7.	Quercetin	0.943	0.598	0.411	0.053	0.348	Yes

Table 6. Toxicity prediction output.

No.	Compound	hERG Blockers	AMES Mutagenicity	Human Hepatotoxicity	Carcinogenicity
1.	Apigenin	0.1	0.618	0.435	0.793
2.	Diphenylcarbazine	0.021	0.981	0.693	0.561
3.	Enamine	0.06	0.44	0.535	0.475
4.	Naringin	0.023	0.939	0.895	0.053
5.	Obovat	0.216	0.698	0.828	0.367
6.	Rutin trihydrate	0.216	0.698	0.828	0.367
7.	Quercetin	0.099	0.657	0.1	0.05

4. Discussion

The potential consequences of anti-cancer drug resistance for the primary treatment for uncomplicated breast cancer. At present, no option exists to combat the pervasive drug resistance. This scenario highlights the imperative for high-throughput screening of phytochemicals to facilitate the advancement of novel anticancer pharmaceuticals. Rutin Hydrate exhibits the greatest potential as an inhibitor, with an

affinity of -9.2 kcal/mol for human placental aromatase. A lower docking score signifies enhanced binding affinity and energy. It is essential to emphasize that these exhibited a higher binding affinity and, therefore, enhanced inhibitory potentials relative to the usual standard ligand. Aromatase belong to the cytochrome P450 (CYP) family enzymes, it converts androstenedione to estrone and testosterone to estradiol (E2) [26]. Aromatase inhibitors block the activity of aromatase, thereby, preventing the synthesis of estrogen, which stimulates the growth and development of breast cancer.

The significant binding affinities demonstrated by the identified compounds indicate their considerable potential to bind to and inhibit human placental aromatase, thereby preventing breast cancer. In this timeframe, the seven selected ligand demonstrated the greatest binding affinity to human placental aromatase, with a docking score from -9.2 to -7.2 kcal/mol.

The main obstacle for medications to be efficiently dispersed throughout the body is their ability to be absorbed in the gastrointestinal system. HIA functions as a metric for forecasting the absorption of a pharmacological molecule in the human intestine post-oral delivery, evaluated via the concentrations of excretion in urine, bile, and feces. The chemical exhibits efficient absorption when at least 90% is assimilated into the human bloodstream [27]. The Caco-2 permeability parameter presents a considerable obstacle for oral drugs, since it entails translocation over the barrier formed by intestinal epithelium generated from human colonic adenocarcinomas, which possess various transport channels [28]. Drugs that have undergone absorption are then disseminated throughout the body. The plasma membrane ATP-binding cassette transporter, P-glycoprotein (P-gp), is crucial in drug transport mechanisms. The activation of P-glycoprotein results in the efflux of the medication from cells, hence hindering the attainment of the therapeutic effect [28]. A crucial element of the distribution process is the drug's ability to traverse the blood-brain barrier (BBB) [29]. The administered medicine is subsequently metabolized. CYP450 participates in the metabolism of pharmaceuticals and xenobiotics in the liver and intestines. When a molecule is recognized as a substrate for at least one CYP450 enzyme, it is anticipated that the compound will be efficiently metabolized by the associated CYP450 enzyme [29]. Drug interactions occur due to the suppression of a particular isoform of the enzyme, resulting in hepatotoxicity [30]. The human liver is the primary site for metabolism, affecting the impact of hazardous substances and many medications. Hepatotoxicity criteria indicate several types of liver damage that may cause organ failure or perhaps result in deadly consequences. Consequently, it is essential to evaluate hepatotoxicity at the development and drug discovery stages for oral delivery [31]. This study illustrated that multiple compounds in the *Uvaria chamae* may function synergistically in treating cancer, owing to their varied mechanisms of action on human placental aromatase and their potential to compete with conventional pharmaceuticals. Moreover, compounds that meet the criteria for drug similarity and have a favorable ADME-T profile can aid in the development of anti-cancer pharmaceuticals produced from *Uvaria chamae*.

5. Conclusion

The study has identified seven compounds that could function as potential anticancer drugs targeting human placental aromatase. Further investigations, encompassing the extraction of these chemicals for in vitro testing, are necessary to validate these findings.

Abbreviations

WHO	World Health Organization
GC-MS	Gas Chromatography-mass Spectrometry
HPLC	High Performance Liquid Chromatography
NIST	National Institute of Standard and Technology
ADMET	Absorption, Distribution, Metabolism, Excretion, And Toxicity
FDA	Food and Drug Administration
HIA	Human Intestinal Absorption

Acknowledgments

I thank AFEAD Biotech Ltd for the service in getting *In-silico* software's for this research.

Author Contributions

Omobolaji Odunowo is the sole author. The author read and approved the final manuscript.

Conflicts of Interest

The author declares no conflicts of interest.

References

- [1] Van Vo, G., Nguyen, T. P., Nguyen, H. T., Nguyen, T. T., Tran, N. M. A., et al. (2022). In silico and in vitro studies on the anti-cancer activity of artemetin, vitexicarpin and penduletin compounds from *Vitex negundo*. *Saudi Pharm. J.* 30 (9), 1301–1314. <https://doi.org/10.1016/j.jsps.2022.06.018>
- [2] World Health Organization (2018). Cancer. https://www.who.int/health-topics/cancer#tab=tab_1 (Accessed on November 19, 2022).
- [3] Akash, S. (2021). An overview of advanced treatment of cancer where are we today. 06.2021-22765836/IJMRE.
- [4] Rahib, L., Smith, B. D., Aizenberg, R., Rosenzweig, A. B., Fleshman, J. M., and Matrisian, L. M. (2014). Projecting cancer incidence and deaths to 2030: the unexpected burden of thyroid, liver, and pancreas cancers in the United States. *Cancer Res.* 74 (11), 2913–2921. <https://doi.org/10.1158/0008-5472.CAN-14-0155>
- [5] Küpeli Akkol, E., Bardakci, H., Barak, T. H., Seker Karatoprak, G., Khan, H., Hussain, Y., et al. (2022). Herbal ingredients in the prevention of Breast Cancer: comprehensive review of potential molecular targets and role of natural products. *Oxid. Med. Cell Longev.* 2022, 6044640. <https://doi.org/10.1155/2022/6044640>
- [6] Majid, R. A., Hassan, H. A., Muhealdeem, D. N., Mohammed, H. A., and Hughson, M. D. (2017). Breast cancer in Iraq is associated with a unimodally distributed predominance of luminal type B over luminal type A surrogates from young to old age. *BMC Women's Health* 17 (1), 27–28. <https://doi.org/10.1186/s12905-017-0376-0>

- [7] Centers for Disease Control and Prevention. (2022). Breast cancer. Available at: https://www.cdc.gov/cancer/breast/basic_info/what-is-breast-cancer.htm [Accessed on November 26, 2022].
- [8] Łukasiewicz, S., Czezelewski, M., Forma, A., Baj, J., Sitarz, R., and Stanisławek, A. (2021). Breast cancer-epidemiology, risk factors, classification, prognostic markers, and current treatment strategies-an updated review. *Cancers* 13, 4287. <https://doi.org/10.3390/cancers13174287>
- [9] Neve, R. M., Chin, K., Fridlyand, J., Yeh, J., Baehner, F. L., Fevr, T., et al. (2006). A collection of breast cancer cell lines for the study of functionally distinct cancer subtypes. *Cancer Cell*. Dec 10(6), 515–527. <https://doi.org/10.1016/j.ccr.2006.10.008>
- [10] Bender, O., and Atalay, A. (2018). Evaluation of anti-proliferative and cytotoxic effects of chlorogenic acid on breast cancer cell lines by real-time, label-free and high-throughput screening. *Marmara Pharm. J.* 22(2), 173–179. <https://doi.org/10.12991/mpj.2018.54>
- [11] American Cancer Society (2022). Breast cancer. Available at: <https://www.cancer.org/cancer/breast-cancer/about/what-is-breast-cancer.html> (Accessed on November 26, 2022).
- [12] Newman, D. J., and Cragg, G. M. (2016). Natural products as sources of new drugs from 1981 to 2014. *J. Nat. Prod.* 79(3), 629–661. <https://doi.org/10.1021/acs.jnatprod.5b01055>
- [13] Küpeli Akkol, E., Guragac Dereli, F. T., Sobarzo-Sánchez, E., and Khan, H. (2020b). Roles of medicinal plants and constituents in gynecological cancer therapy: current literature and future directions. *Curr. Top. Med. Chem.* 20(20), 1772–1790. <https://doi.org/10.2174/156802662066200416084440>
- [14] Cragg, G. M., and Pezzuto, J. M. (2016). Natural products as a vital source for the discovery of cancer chemotherapeutic and chemopreventive agents. *Med. Princ. Pract.* 25(2), 41–59. <https://doi.org/10.1159/000443404>
- [15] Sehrawat, R., Rathee, P., Akkol, E. K., Khatkar, S., Lather, A., Redhu, N., et al. (2022). Phenolic acids-versatile natural moiety with numerous biological applications. *Curr. Top. Med. Chem.* 22(18), 1472–1484. <https://doi.org/10.2174/1568026622066220623114450>
- [16] Küpeli Akkol, E., Genc, Y., Karpuz, B., Sobarzo-Sánchez, E., and Capasso, R. (2020a). Coumarins and coumarin-related compounds in pharmacotherapy of cancer. *Cancers* 12, 1959. <https://doi.org/10.3390/cancers12071959>
- [17] Saibabu, V., Fatima, Z., Khan, L. A., and Hameed, S. (2015). Therapeutic potential of dietary phenolic acids. *Adv. Pharmacol. Sci.* 2015, 823539. <https://doi.org/10.1155/2015/823539>
- [18] Cragg, G. M., and Newman, D. J. (2005). Plants as a source of anti-cancer agents. *J. Ethnopharmacol.* 100(1-2), 72–79. <https://doi.org/10.1016/j.jep.2005.05.011>
- [19] Mabberley DJ (2008) *Mabberley's Plant-Book: A portable dictionary of plants, their classification and uses.* 3rd edn. Cambridge University Press, Cambridge, UK. 1021p. (PDF)
- Acanthus montanus* (Nees) T. Anderson: Review. Available from: https://www.researchgate.net/publication/365941573_Acanthus_montanus_Nees_T_Anderson_Review [accessed Jan 29 2025].
- [20] Mildawati M, Sobir S, Sulistijorini S, Chikmawati T (2022) Metabolite profiling of *Davallia* in The Mentawai Islands, West Sumatra, Indonesia. In: Proceedings of the 7th International Conference on Biological Science (ICBS 2021). *Adv Biol Sci Res* 22: 66–72. <http://dx.doi.org/10.2991/absr.k.220406.010>
- [21] Chen G, Seukey AJ, Guo M (2020) Recent advances in molecular docking for the research and discovery of potential marine drugs. *Mar Drugs* 18(11): 545. <https://doi.org/10.3390/md18110545>
- [22] Sasidharan et al., *Afr J Tradit Complement Altern Med.* (2011) 8(1): 1-10.
- [23] Ghosh, D. Novel aromatase inhibitors by structure –guided design. (2012) *J. Med. chem.* 55: 8464-8476.
- [24] Trott O, Olson AJ. AutoDock Vina: improving the speed and accuracy of docking with a new scoring function, efficient optimization, and multithreading. *J Comput Chem* 2010 Jan 30; 31(2): 455–61. <https://doi.org/10.1002/jcc.21334>
- [25] ADMETlab 2.0 <https://admetmesh.scbdd.com/>
- [26] Dutta U & Pant K 2008 Aromatase inhibitors: past, present and future in breast cancer therapy. *Medical Oncology* 25 113–124.
- [27] Borad MA, Jethava DJ, Bhoi MN, Patel CN, Pandya HA, Patel HD (2020) Novel isoniazid-spirooxindole derivatives: design, synthesis, biological evaluation, in silico ADMET prediction and computational studies. *J of Mol Struct* 1222: 128881.
- [28] Pham The H, González-Álvarez I, Bermejo M, Sanjuan VM, Centelles I, Garrigues TM, Cabrera-Pérez MA (2011) In silico prediction of Caco-2 cell permeability by a classification QSAR approach. *Mol Inf* 30: 376–385.
- [29] Babatomiwa K, Joseph AO, Damilohun SM, Olaposi IO, Niyi SA (2020) Virtual screening and pharmacokinetic studies of potential MAO-B inhibitors from traditional Chinese medicine. *J Biol Eng Res Rev* 7(1): 8–15.
- [30] May M, Schindler C (2016) Clinically and pharmacologically relevant interactions of antidiabetic drugs. *Ther Adv Endocrinol Metab* 7(2): 69–83.
- [31] Ojo A, Ojo AB, Okolie C, Nwakama MAC, Iyobhebhe M, Evbuomwan IO, Nwonuma CO, Maimako RF, Adegboyega AE, Taiwo OA, Alsharif KE, Batiha GES (2021) Deciphering the interactions of bioactive compounds in selected traditional medicinal plants against Alzheimer's diseases via pharmacophore modeling, auto-QSAR, and molecular docking approaches. *Molecules* 26(7): 1996.